A COMPARATIVE STUDY ON HYDRAULIC FEATURES OF SUPERCRITICAL WATER NATURAL AND FORCED CIRCULATION LOOPS

KUANG Bo[1], DU Li-Guo[2]
[1] School of Nuclear Science and Engineering, Shanghai Jiao Tong University, Shanghai, China
[2] East China Electric Power Design Institute, Shanghai, China

Abstract

With establishment of a unified hydraulic model for both natural and forced circulation loops, and with considering the unique variation of thermo-physical properties at supercritical pressures, along with the nonlinear momentum transport and system coupling characteristics, this paper, by applying appropriate nonlinear numerical computation based on continuation concept, presents a comparative study on the complex hydraulic features of both supercritical water systems. Special non-monotonic relationships of mass-flow rate vs. heating power of both natural and forced circulations are comparatively investigated. Meanwhile, effects of such factors as inlet bulk temperature of heating section, local resistances and/or pump characteristics on system hydraulic and heat transmission features are delivered. Furthermore, characteristics of forced circulation driven by both a real and ideal pump are compared.

Keywords: Supercritical pressure, Non-linear hydraulic features, Natural circulation, Forced circulation.

1. Introduction

Under supercritical pressures, fluid thermodynamic and transport properties, such as specific heat, specific volume, heat conductivity and viscosity etc., experience drastic yet continuous variations near the pseudo-critical point, by which significant effects of the heat load and buoyancy in heated region on flow and heat transfer characteristics are brought about. Under certain conditions, such various transport mechanisms as anisotropic turbulence, laminarization etc. and unique phenomena as heat transfer deterioration (HTD) are observed. It is, therefore, expected that, for flow near pseudo-critical point, distinct features of parameter distribution from multi - parametric coupling and combined effects of local heat and momentum transport lead to prominent characteristics other than normal subcritical flow, exhibiting complex “multi-fluid” effect of “light-heavy-fluid mixing”. Meanwhile, strong nonlinear coupling between driving force and resistance integrated along the loop also contributes to special systematic hydraulic features of circulation. It is recommended that all the above mentioned influences have to be considered while analyzing system behavior under supercritical pressures. And through applying flow and heat transfer correlations reflecting the complicated effects across pseudo-critical point and properly integral modeling of the system, special hydraulic characteristics and engineering essence of water circulation are expected to be reasonably simulated and understood.

In this paper, both a simplified forced and a natural circulation water loop under supercritical pressures are comparatively studied. With the combination of property variation and transport features into analytical thermo-hydraulic model and by applying proper nonlinear numerical method, hydraulic mechanism and related parametric effects of the systems are preliminarily investigated.

2. Description and Hydraulic Modeling of a Single-Channel Circulation under Supercritical Pressure

2.1 Brief Introduction to the Loops

Figure 1 presents schematic diagrams of single-channel water loop of both natural circulation (a) and forced one (b). The forced loop consists of a lower horizontal section, a circulation pump, a vertical heating section, a riser, an upper horizontal section, a cooling section (horizontally located), a pressure controller and a downcomer. In the natural circulation loop, structure of the loop is almost the same, except that circulation pump is missing (yet local loss of the pump is still preserved for reasonably comparison).

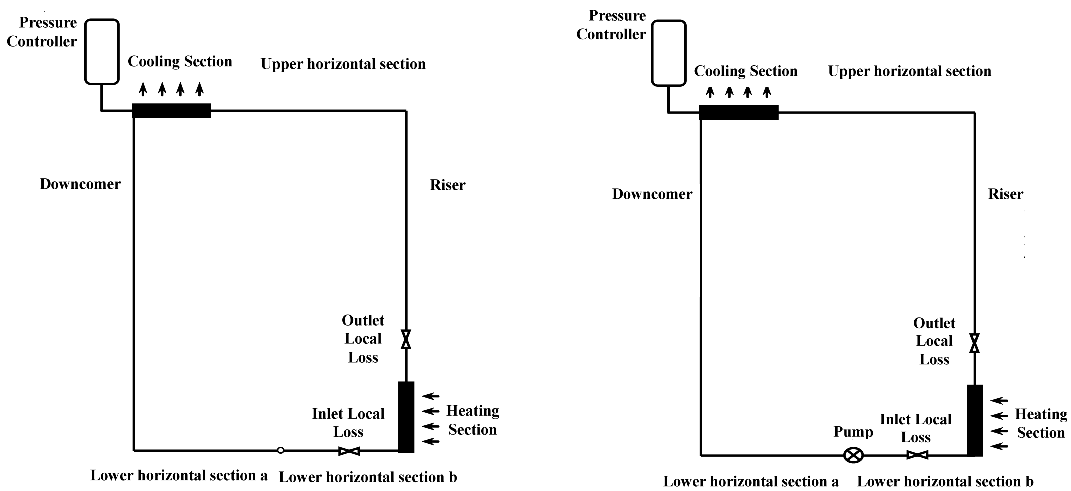

a Natural Circulation b Forced Circulation

Figure 1 Schematic Diagram of Single-Channel Water Loops under Supercritical Pressures

2.2 Steady State Models for Forced and Natural Circulation

2.2.1 Simplifications and Model Equations

In this paper, following assumptions are adopted for simplified analysis:

(1) Static One-dimensional flow assumption, ie. parameters on the cross-sections perpendicular to the loop direction are assumed homogeneously distributed;

(2) Thermal effects of friction and axial heat conduction of fluid neglected;

(3) Ideal pressure controller hypothesis, ie. local pressure value at the connection of controller and loop keeps constant;

(4) Evenly distributed heating load and cooling heat flux assumption, in addition to the cooling power equaling to the heating power and the rest parts being adiabatic;

(5) Point pressure head source of the pump assumed, with given pressure head - mass flow-rate characteristics.

Keeping these in mind, basic steady state control equations for both natural and forced circulations are as follows:

Mass equation
$$\frac{dG}{dz} = 0 \tag{1}$$

Momentum equation
$$\frac{d\left(G^2/\rho\right)}{dz} = -\frac{dP(z)}{dz} - \rho g \sin\theta - f(z) \tag{2}$$

Energy equation
$$G\frac{dH(z)}{dz} = q(z) = \begin{cases} q_h = \dfrac{Q}{L_h}, & \text{Heating Section} \\ 0, & \text{Adiabatic Sections} \\ -q_c = -\dfrac{Q}{L_c}, & \text{Cooling Section} \end{cases} \tag{3}$$

in which, G denotes circulation mass flow-rate, z the one-dimensional coordinate along the loop length, $P(z)$ pressure distribution along z, θ the inclination angles of various sections (for horizontal section, $\theta = 90°$; and for vertical section, $\theta = 0°$); $f(z)$ represents hydraulic resistance per length in various sections, including frictional resistance and local resistance, ie. $f(z) = f_{\text{fr}}(z) + f_{\text{l}}(z)$; $H(z)$ enthalpy distribution along z; $q(z)$ stands for heating and cooling load (per length) on the sections, while as q_{h} for heating and q_{c} for cooling; Q is the total heating power, and, L_{h} and L_{c} the length of heating and cooling sections, respectively.

Integrating the momentum equation (2) along the loop, we have

$$G^2 \oint_{\text{Loop}} d\left(\frac{1}{\rho}\right) = -\oint_{\text{Loop}} dP - \oint_{\text{Loop}} \rho g \sin\theta dz - \oint_{\text{Loop}} f d\! \tag{4}$$

and,

$$\oint_{\text{Loop}} dP = \begin{cases} -\Delta P_{\text{pump}}, & \text{for forced circulation} \\ 0, & \text{for natural circulation} \end{cases} \tag{5}$$

driving force for the loop then writes

$$-\oint_{\text{Loop}} dP - \oint_{\text{Loop}} \rho g \sin\theta dz \equiv F_{\text{drive}}(G, Q)$$

and loop resistance is

$$\oint_{\text{Loop}} f dz \equiv F_{\text{resist}}(G\ Q)$$

The static loop driving force - resistance balance equation is written as

$$\Lambda(G, Q) = F_{drive}(G, Q) - F_{resist}(G, Q) = 0 \tag{6}$$

Therefore, studying the system steady state hydraulic problem turns out to solving the driving force - resistance balance equation (6) with restriction of eq. (1) and (2). In numerical aspect, related discrete forms of eq. (1), (3) and (6) are written as

$$G_i = G \tag{7}$$

$$G_i\left(H_i - H_{i-1}\right) = q_i \Delta z \tag{8}$$

$$\begin{aligned} &\Delta p_{\text{pump}} + g\left(\frac{H_{i+1}\rho_{i+1} + H_i\rho_i}{H_{i+1} + H_i}\right)\Delta z \sin\theta \\ &= \sum_{i=1}^{N} \xi_{\text{fr},i+1} \frac{\Delta z}{D_i}\frac{G_i^2}{\rho_i + \rho_{i+1}} + \sum_{i=1}^{N} \xi_{1,i+1}\frac{G_i^2}{2\rho_{i+1}} \end{aligned} \tag{9}$$

where, the subscript "*i*" denotes node number; ξ_{fr} is frictional resistance coefficient, while ξ_{l} local resistance coefficient; D is the hydraulic diameter; ΔP_{pump} represents the driving head by circulation pump and for natural circulation, $\Delta P_{\text{pump}} = 0$. It is further mentioned eq. (9) is for the case that channel diameters of all loop sections are identical.

Compared with those on heat transfer, relatively scarce study on frictional resistance correlations of water under supercritical pressures is found in available references. In this calculation, therefore, Kondrat′ev correlation is for the present study applied for adiabatic sections, while Filonenko correlation for non-adiabatic sections (I. L. Pioro *et al*, 2004).

2.2.2 Numerical Algorithm

For simplification, the axial heat flux within the heating and cooling section is assumed evenly distributed, which implies that, fluid enthalpy in z direction is linearly distributed. Temperature and density, however, still present strong nonlinear distribution due to abrupt variation of properties in the region about pseudo-critical point. And thus, strong nonlinear characteristics of the integrated driving force $F_{\text{drive}}(G, Q)$ and resistance $F_{\text{resist}}(G, Q)$ are still expected, which are, in the meanwhile, closely coupled. Therefore, the global static hydraulic features of both forced and natural circulations under supercritical pressures attribute to characteristics of the solution family of nonlinear parameter equation (6), under the restriction, of course, of eq. (1) and (3). And for solving the equation, appropriate nonlinear numerical method should be introduced.

A numerical algorithm based on continuation concept (M. Kubicek and M. Marek, 1983) is applied for solving nonlinear equation (6). Solution scheme starts from any point within the solving domain without rigorous restriction on initial value for iteration, which is in favor of solving nonlinear equation in large range. With the algorithm, relation between mass flow-rate G and heating power Q is expected to be acquired, avoiding to a great extent the phenomena of non-convergence or missing of solution. A schematic description of the approach is as following:

Let the equilibrium solution set of $\Lambda(G, Q) = 0$ be a continuous, smooth curve in space (G, Q), arc length of the curves being one of the parameters. Differentiate with relative to s on both sides of the equation leads to

$$\frac{d\Lambda}{ds} = \frac{\partial\Lambda}{\partial G}\frac{dG}{ds} + \frac{\partial\Lambda}{\partial Q}\frac{dQ}{ds} = 0 \tag{10}$$

Meanwhile, a priori relation is used, which writes:

$$\frac{dG}{ds}+\frac{dQ}{ds}=1 \tag{11}$$

Through (10) and (11), slope of the curve (dG/dQ) is acquired. Based on this, the initial values for iteration are obtained by Newton approach, any values along the curve are then numerically computed through explicit Adams-Bashforth method. And thus is the global equilibrium solution deduced.

2.2.3 Thermodynamic Conditions and Geometry Parameters for Calculation

In this paper, thermodynamic conditions for calculation are: inlet temperature of the heating section keeps 280°C for basic calculation case; pressure at the location of pressure controller - loop connection keeps constant of 25MPa. As for geometry parameters of calculation, diameters of all sections are 0.026m; lengths of composed pipes in the loop and related node partition for calculation are given in Table 1.

Table 1 Lengths of Composed Pipes in Loop and Nodalization

Location		**Length, m**	**Number of nodes**
downcomer		10	100
riser		9	90
heating section		1	50
cooling section		1	50
horizontal section	lower section 1	1	10
	lower section 2	2	20
	upper section	2	20

2.2.4 Circulation Pump Models for comparative calculation

In order to understand influence of pump characteristics on hydraulic behavior of forced circulation under supercritical pressures, 5 typical flow rate - pressure head (*G*-*h*) relations of circulation pump are selected for comparative calculation, which are shown in two pump groups in Figure 2, denoted and distinguished as pump $1^{\#}$~$5^{\#}$ respectively. Among the pumps, pump $2^{\#}$ is regarded as the basic pump for comparison. Since flow-rate in the loop under supercritical pressure is relatively low, all the adopted pumps $1^{\#}$~$5^{\#}$ belong to low specific speed pump. It should also be mentioned that, in order to better understand coupling characteristics of circulation loop and pump behavior, all the selected pumps are non-hump type pumps so that other possible effects arisen from hump feature might be avoided. Furthermore, a pump $6^{\#}$ is defined, which is actually an ideal pump with constant pressure head. Therefore, there are altogether 3 groups for comparative calculation: pump group I consists of pump $1^{\#}$, $2^{\#}$ and $3^{\#}$ with identical slope but different pressure head with respect of the same flow-rate (for observing the influence of effective pump power on forced circulation); pump group II, in contrast, includes pump $4^{\#}$, $2^{\#}$ and $5^{\#}$ with different slope (reflecting different self-adjusting capability of pressure head) but small variation in pressure head (for approximately evaluating the influence of pressure head self-adjusting capability on forced circulation); and pump group III, consisting of pump $2^{\#}$ and $6^{\#}$, is used to compare the hydraulic difference of made by practical and ideal pumps.

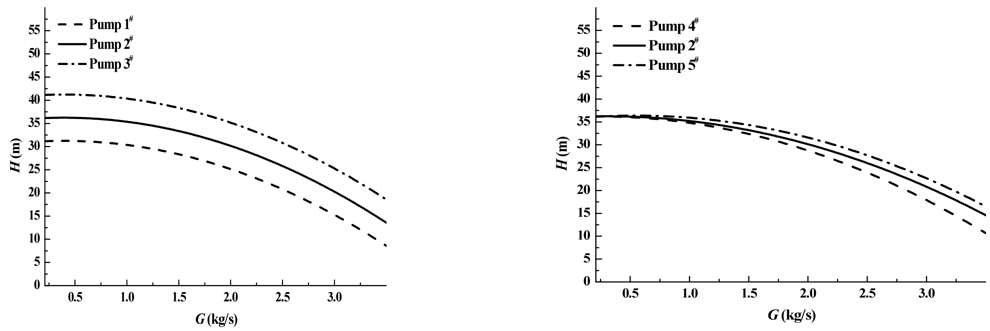

a Pump group I **b Pump group I**

Figure 2 *G* - *H* Characteristics of the Pumps Adopted in the Present Calculation

3. Analysis on the Results

3.1 Hydraulics and Heat Transport Characteristics of Natural Circulation under Supercritical Pressures

3.1.1 <u>Characteristics of Driving Force, Hydraulic Resistance and Flow-rate - Heat Load Relation</u>

3.1.1.1 <u>Driving Force and Resistance</u>

Nonlinear trends of buoyancy driving force and flow resistance change with heating power variation at different flow-rates are demonstrated in Figure 3.

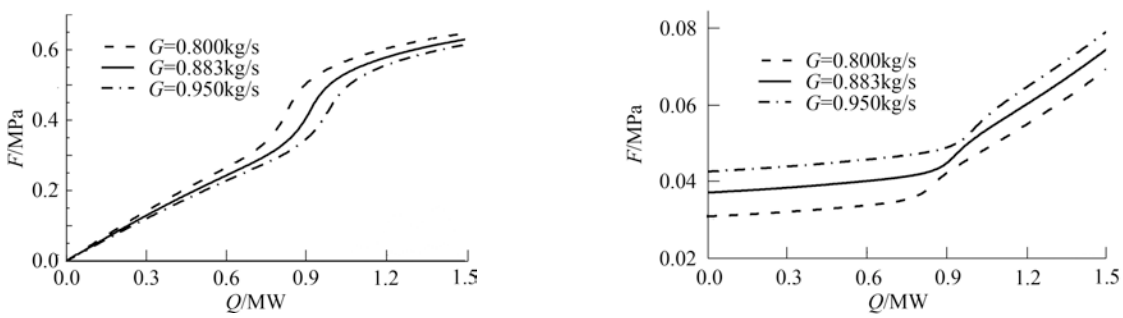

a Driving Force - Heating Power Relation b Resistance - Heating Power Relation

Figure 3 Buoyancy Driving Force, Resistance -Heating Power Relations at Different Flow-Rates

It is found that driving force and flow resistance vary with heating power monotonously for all natural circulation flow-rates. The higher flow-rate is, the smaller driving force and the larger resistance are observed. There exists a "transition region" for both driving force and flow resistance. In region of far smaller heating power than transition region, driving force increases fast with heating power and resistance increases slowly, while in region of far higher heating power, driving force increases slowly and resistance increases rapidly. And within the transition region, both driving force and resistance increase sharply with heating power.

Since riser 4 is far longer than heating section 3 and fluid density ρ_1 in downcomer 1 is approximately constant, driving force $\oint_{\text{Loop}} \rho g \sin\theta dz$ is primarily determined by density of water in riser (also, exit density of heating section ρ_3). Then approximately we have: F_{drive} is proportional to $\left[\rho_1 - \rho_3\left(h_3\right)\right]$, in which h_3 is exit enthalpy of the heating section. Assume evenly heating and constant G, then $h_3 \propto q \propto Q$. Therefore, $F_{\text{drive}} \propto \left[\rho_1 - \rho_3\left(Q\right)\right]$. While ρ_3-Q relation corresponds to density- enthalpy relation under supercritical pressures, the "transition region" of driving force corresponds to the condition that pseudo-critical points under related pressures are observed around the exit of heating section.

Considering that adiabatic section is far longer than heating length plus cooling section and that $\oint_{\text{Loop}} f\, dz \propto \oint_{\text{Loop}} \xi \frac{G^2}{2\rho} dz$, it is approximately regarded that loop impedance is mainly dependent on that of adiabatic sections. While thermodynamic state and properties in downcomer 4 and lower horizontal section almost keeps constant, total variation of loop resistance is mainly decided by the resistance change of riser 4 and upper horizontal section 5. For a certain G, it is found from the Kondrat′ev correlation that $\xi \propto \text{Re}^{-0.22} \propto \mu^{0.22}$ so that, approximately, $F_{\text{resist}} \propto \mu^{0.22}\rho^{-1.0}$. And for water under supercritical pressures, μ is far smaller than ρ in value. And thus $F_{\text{resist}} \propto \rho^{-1.0}$, namely, $F_{\text{resist}} \propto \upsilon$ (υ is specific volume of water). In riser 4 and upper horizontal section 5, fluid properties are regarded as almost the same as those at the outlet of heating section 3. Therefore, trend of loop resistant variation is similar to that of specific volume-temperature relation under supercritical pressures. And the "transition region" of resistance corresponds to the condition that pseudo-critical points under related pressures are observed around exit of heating section.

3.1.1.2 Flow-rate vs. Heat Load Relation

Under supercritical pressures, properties of fluid vary abruptly around pseudo-critical point. With heating power as parameter, hydraulic characteristics are therefore controlled by the loop driving force- resistance balanced equation (6).

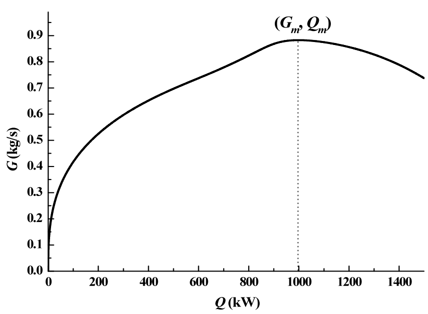

Figure 4 Flow-Rate vs. Heating Power Relation in Natural Circulation

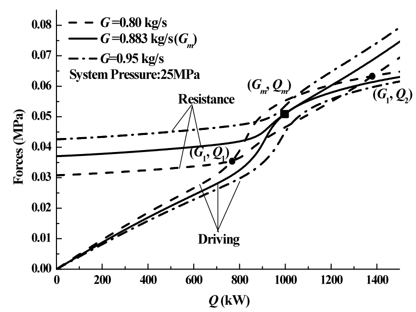

Figure 5 Driving Force and Resistance vs. Heating Power in Natural Circulation

Figure 4 demonstrates the relation of natural circulation flow-rate G vs. heating power Q under the basic calculation condition. It is found that G firstly increases and then decreases with Q increasing, a maximum G_m being reached at Q_m. This implies that for a certain value of G, there might be two corresponding Q values, which is determined by features of nonlinear driving force and resistance functions coupling. As indicated by Figure 5, steady state solution of circulation flow-rate by eq. (6) corresponds to the intersection (or tangent) points of driving force curve and resistance curve. There exist three possibilities, intersecting at two points, tangent at one point, and no intersection. In Figure 5, for example, two intersections are obtained when flow-rate is 0.80kg/s, which means that natural circulation flow-rate of 0.80kg/s can be caused by both heating powers of Q_1 and Q_2. This is the multi-solution situation for eq. (6), which obviously reflects the competition between buoyancy driving force and resistance. When flow-rate is 0.883kg/s (Q_m), the driving force curve and resistance curve become tangent, the related flow-rate G_m (0.883kg/s) reaches the highest and only one Q (Q_m) solution is available. And for flow-rate of 0.95kg/s, no intersection is found, which means that 0.95kg/s is not practically attainable for present natural circulation loop. Further, calculated data show that Q_m corresponding to G_m turns to be the heating power that makes outlet parameters right within the property abruptly varying pseudo-critical region (see Figure 6 and 7).

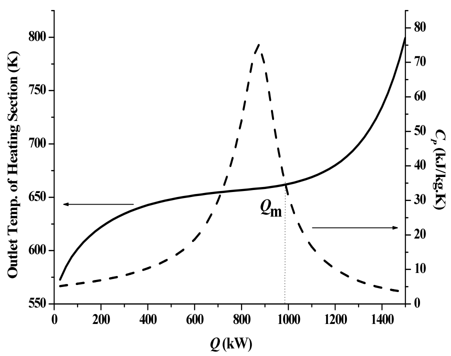

Figure 6 Outlet Temperature of Heating Section v.s. Heating Power Relationships and Related Bulk Property C_p Variation

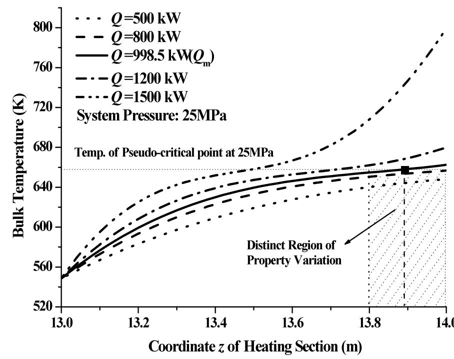

Figure 7 Temperature Distribution within Heating Section at Different Heating Power

3.1.2 <u>Heat Transport Characteristics</u>

As demonstrated in Figure 8, two typical regions with different natural circulation features of heat transport are identified: In $Q < Q_m$ region, Q increases with G increasing, which is favorable for local heat transfer and system heat transport, while in $Q > Q_m$ region, G decreases with Q increasing, which leads to adverse situations, such as local heat transfer deterioration (HTD) or adverse loop heat transport characteristics. In addition, related reference (G. R. Dimmick and V. Chatoorgoon, 1985) pointed out that dynamic instabilities might probably happen in $Q > Q_m$ region. Therefore, from the viewpoint of safe heat transfer and of operation, Q_m is proposed to be an dividing and limiting value for favorable and unfavorable heat transport of natural circulation under supercritical pressures. In practice, system is recommended to operate in $Q < Q_m$ region for safety.

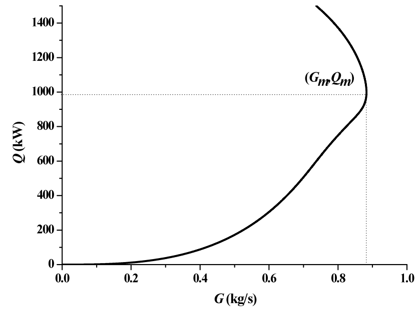

Figure 8 Heat Transport Power vs. Flow-Rate in Natural Circulation

3.2 Hydraulic and Heat Transport Characteristics of Forced Circulation under Supercritical Pressures

3.2.1 Driving Force, Resistance and Flow-Rate vs. Heat Load Relation

3.2.1.1 Driving Force and Resistance Characteristics

Trends of driving force and hydraulic resistance variation with heating power are presented in Figure 9a and 9b. It is observed that:

(1) Both driving force and resistance increase monotonously with heating power;

(2) Driving force decreases with flow-rate increasing, while resistance increases;

(3) There exists a transition region on both sides of which driving force and resistance variations with heating power behave differently.

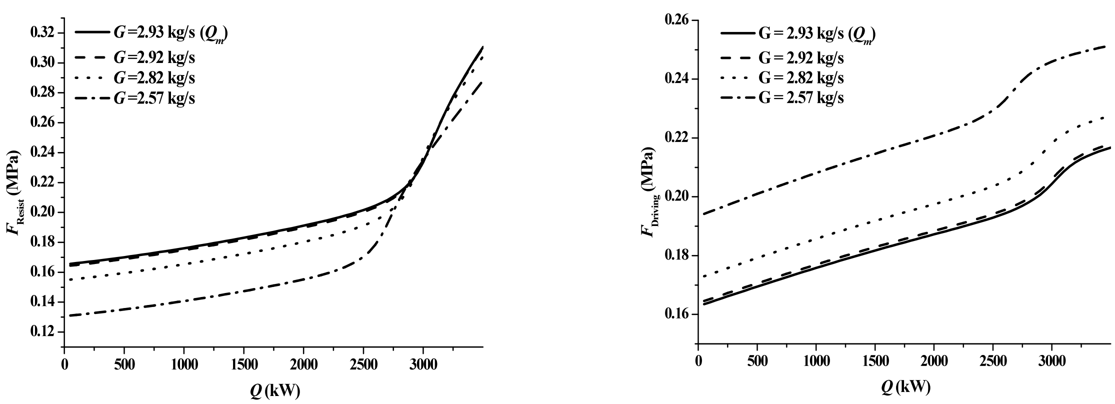

a Driving Force - Heating Power Relations b Resistance - Heating Power Relations

Figure 9 Trends of Driving Force and Flow Resistance Variations with Heating Power at Different Flow-Rates in Forced Circulation

3.2.1.2 Flow-Rate vs. Heat Load Relation

Figure 10 shows the *G*-*Q* relation of forced circulation in which pump $2^{\#}$ is applied for basic condition calculation. Obviously, both flow-rate and heating power in forced circulation are far higher than those in natural circulation for sake of the existence of circulation pump. The buoyancy-resistance competition resulted multi-solution feature in natural circulation is also observed, but with much less dominant. Instead, it is noted that there exist two distinct regions of *G*-*Q*: when heating power is relatively low ($Q < Q_d$, $Q_d \sim 2800$kW), a rather "flat" multi-solution region of flow-rate with a maximum G_m is observed; when heating power becomes larger ($Q > Q_d$), an abrupt drop of flow-rate which is determined by pump characteristics is identified. Interaction between driving force (buoyancy plus pump driving head) and resistance that causes formation of such special hydraulic characteristics is illustrated in Figure 11.

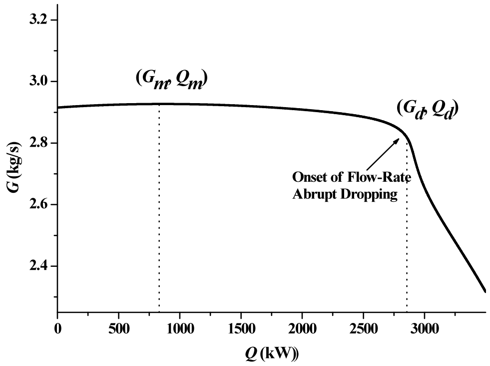

Figure 10 *G* - *Q* Relation of Forced Circulation

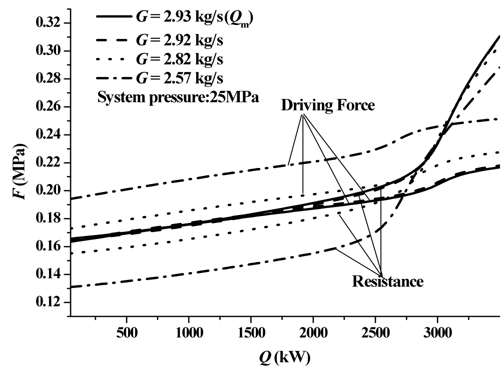

Figure 11 Driving Force and Flow Resistance vs. Heating Power in Forced Circulations

Calculation also indicates that, for forced circulation, it is Q_d corresponding to G_d, rather than Q_m related to G_m that turns to be the heating power that makes outlet parameters right within the abruptly varying pseudo-critical region.

3.2.2 Heat Transport Characteristics

Basically, when $Q < Q_d$, forced circulation flow-rate is relatively high and varies little with heating power increasing. This is the region where pump is capable of adjusting and controlling, and of course, where the region is heat transfer and heat transport favorable. When $Q > Q_d$, however, it is out of the capability of pump dominant. The loop is under low flow-rate, high heat load condition, which is rather unfavorable for local heat transfer and global heat transport.

4. Parametric Effects

4.1 Loop Height Effect

Provided that length of heating section (heat load) keeps unchanged, it is demonstrated in Figure 12 and 13 that natural circulation flow-rate *G* increases with loop (riser) height increasing. Meanwhile, effect of loop height on outlet temperature is also observed: the higher the loop is, the lower outlet temperature is observed. And this riser effect seems significantly amplified in region $Q > Q_m$, in which water from the outlet is already completely post pseudo-critical. Property effect is dominant in natural circulation.

As for forced circulation, as shown in Figure 14 and 15, flow-rate *G* decreases with loop height increasing, and it is only after the abrupt dropping region of *G* (after (G_d, Q_d)) that noticeable loop height effect on outlet temperature is observed. This implies that whenever it is within the region that pump is capable of adjusting, outlet temperature is pump-dominating.

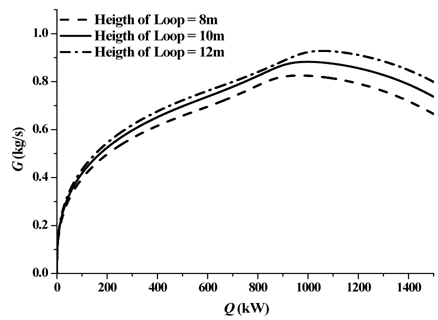

Figure 12 Effect of Loop height on Flow-Rate in Natural Circulation

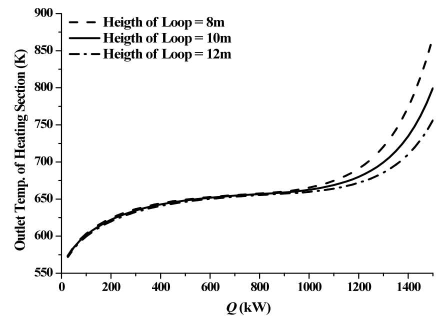

Figure 13 Effect of Loop Height on Outlet Temp. of Heating Section in Natural Circulation

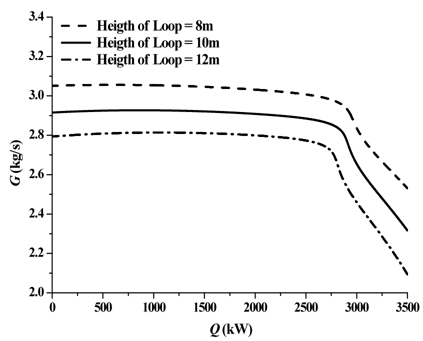

Figure 14 Effect of Loop height on Flow-Rate in Forced Circulation

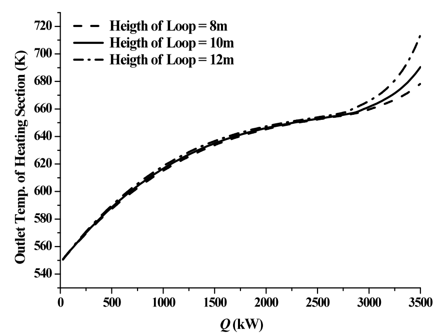

Figure 15 Effect of Loop Height on Outlet Temp. of Heating Section in Forced Circulation

4.2 Inlet Temperature Effect

Figure 16 presents inlet temperature influence of heating section on natural circulation flow-rate G. It is indicated that, lower inlet temperature corresponds to higher maximum natural circulation flow-rate G_m and higher Q_m (provided that no deficient heat transfer problem is met). In another word, natural circulation capability (potential) tends to be larger for low inlet temperature condition.

Effect of inlet temperature on outlet temperature in natural circulation is demonstrated in Figure 17. It seems that difference in both flow-rate and outlet temperature by inlet temperatures is relatively limited in $Q < Q_m$ region, while in $Q > Q_m$ region the difference is more and more amplified as Q increases. And for some high inlet temperature cases in $Q > Q_m$ region, considerably large outlet temperature rise might be observed, which is quite dangerous for stability and operation safety considering the decrease trend of G with Q right in this region.

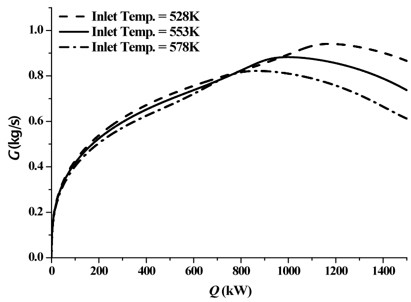

Figure 16 Effect of Inlet Temp. of Heating Section on Flow-Rate in Natural Circulation

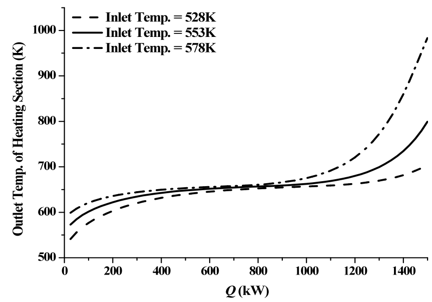

Figure 17 Effect of Inlet Temp. of Heating Section on Outlet Temp. in Natural Circulation

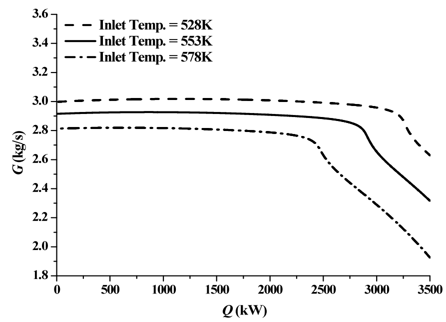

Figure 18 Effect of Inlet Temp. of Heating Section on Flow-Rate in Forced Circulation

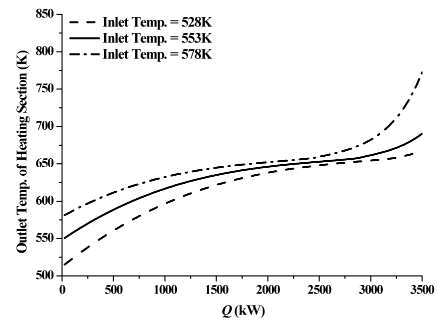

Figure 19 Effect of Inlet Temp. of Heating Section on Outlet Temp. in Forced Circulation

For forced circulation, it is seen from Figure 18, 19 that, flow-rate decreases, outlet temperature increases with inlet temperature increasing. Meanwhile, the abrupt flow dropping point G_d in forced circulation occurs earlier with inlet temperature increasing.

This is easy to understand: since outlet temperature of heating section increases with inlet temperature increasing, fluid density in riser that follows the heating section will decrease, which leads to higher loop resistance. To balance the higher pressure drop by this effect, lower loop flow-rate is coupled so that larger driving force is provided by the pump, and thus, for a specific pump, is the condition out of pump adjusting capacity earlier reached. Therefore, for forced circulation, higher inlet temperature may cause enlarged unfavorable region for heat transfer (flow-rate dropping region), which reduces safety performance of the loop.

4.3 Local Loss Effect

Local form loss obviously leads to lower flow-rate and higher outlet temperature in both natural and forced circulations with the same heating power. However, impacts of entrance and exit local resistances are different, that of exit local resistance being more significant and more and more amplified in the post-pseudo-critical region ($Q > Q_m$ for natural circulation; or $Q > Q_d$ for forced circulation). Trends of local resistance effect in both natural and forced circulations are shown in Figure 20 ~ 24.

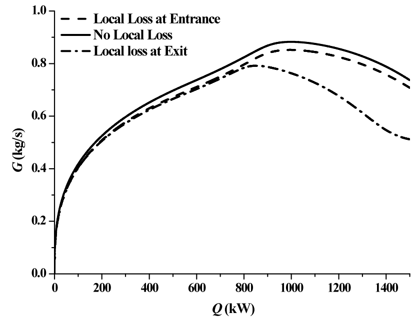

Figure 20 Effect of Local Losses on Flow-Rate in Natural Circulation

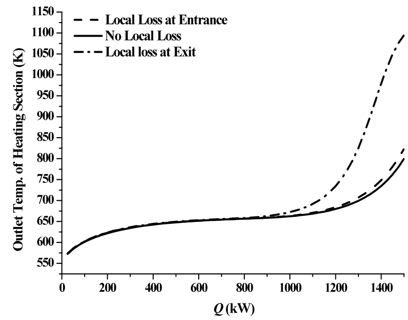

Figure 21 Effect of Local Losses on Outlet Temp. of Heating Section in Natural Circulation

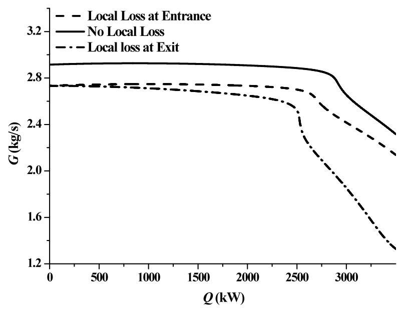

Figure 22 Effect of Local Losses on Flow-Rate in Forced Circulation

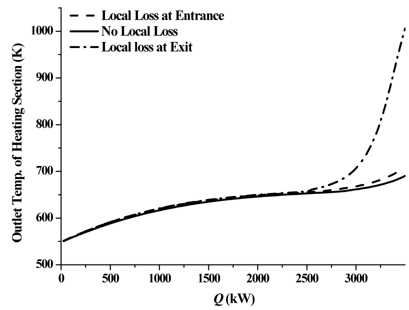

Figure 23 Effect of Local Losses on Outlet Temp. of Heating Section in Forced Circulation

4.4 Pump Effect on Forced Circulation G - Q Relation

4.4.1 Influence of Pump Effective Power

Figure 24 demonstrates trends of *G* - *Q* relations using pumps $1^{\#}$, $2^{\#}$ and $3^{\#}$ of different effective powers or heads (pump group I). It is concluded that for pump group I which is of the same pump characteristics but different effective powers or heads, circulation flow-rate *G* increases with pump head increasing, and abrupt drop points of flow-rate increases in turn. Therefore, it may be concluded that increasing effective power or head of pump is favorable for heat transfer and heat transport in forced circulation.

4.4.2 Influence of Slope of Pump Characteristic Curve

Figure 25 presents trends of *G* - *Q* relations using pumps $4^{\#}$, $2^{\#}$ and $5^{\#}$ with different slopes of pump characteristic curve (pump group II). It is seen that, under the condition of similar pump effective power but with smaller slopes of characteristic *G-H* curve (larger self-adjusting capability), circulation flow-rate *G* tends to get higher. Thus can one conclude that it is more favorable for loop heat transport with smaller slope in pump characteristic curves.

Figure 26 indicates influences of real and ideal pump (pump $2^{\#}$ and $6^{\#}$) on mass flow-rate. It is obviously that circulation flow-rate gets much higher for ideal pump, where the characteristic curve slope is zero and *G-H* self-adjusting capability is infinitely large. Moreover, much higher heating power might be added to approach the abrupt drop point of mass flow-rate using an ideal pump.

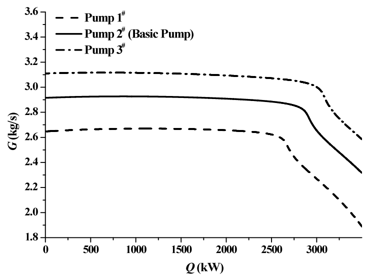

Figure 24 Effect of Pump Effective Power on Flow-Rate in Forced Circulation

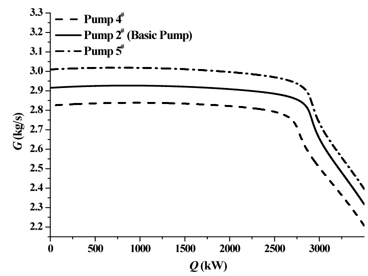

Figure 25 Effect of Slope of Pump Characteristic Curve on Flow-Rate in Forced Circulation

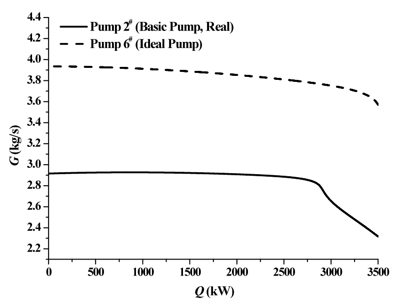

Figure 26 Effect of Real and Ideal Pump on Flow-Rate in Forced Circulation

5. Conclusions

A unified one-dimensional steady state hydraulic model of both a natural and a forced circulation water loop under supercritical pressure is established. Considering its special property variation and nonlinear resistance features, hydraulic characteristics, heat transport capability and parametric effects of both natural and forced circulation loops under supercritical pressure are investigated through a nonlinear numerical algorithm. Following conclusions are drawn, for which further experimental validation is preferable:

(1) A specific feature of flow-rate - heat load relation of natural circulation under supercritical pressure is revealed. Flow-rate in the loop first increases and then decreases rapidly with heating power and reaches it maximum G_m at certain heating power Q_m. Favorable operating region for local heat transfer and loop heat transport is found to be within range of $Q < Q_m$. In contrast, mass flow-rate in forced circulation experiences first a nearly flat region followed with an abrupt drop one with heating power increases. Adverse condition in abrupt dropping region of mass flow-rate may possibly impair loop heat transport and operation safety.

(2) For natural circulation, both higher inlet temperature and local loss lead to flow-rate decreasing and make outlet temperature increase. Among the influences of inlet and exit local loss, the latter tends to be larger. For forced circulation, trends of inlet temperature and local loss effects on system hydraulic features are similar.

(3) In forced circulation, pump characteristics have obvious influences on system hydraulics and heat transport. Higher circulation flow-rate might be obtained through either increasing pump effective power or decreasing the slope of G - H curve. These strategies are also beneficial for loop heat transport.

6. Acknowledgment

This work is financially supported by "National Basic Research Program of China" (No. 2007CB209804).

7. References

[1] Pioro I. L., Duffey R. B. and Dumouchel T. J., "*Hydraulic Resistance of Fluids Flowing in Channels at Supercritical Pressures* (*Survey*)", Nuclear Engineering and Design, Vol. 231, Iss. 2, 2004, pp187-197.

[2] Dimmick G. R. and Chatoorgoon V., "*Experimental and Analytic Investigation of Two-Phase Stability in a Natural Circulation Loop*", ASME 85-WA/HT-16, ASME Winter Meeting, Nov., 1985.

[3] Kubicek M. and Marek M., "*Computational Methods in Bifurcation Theory and Dissipative Structures*", Spring-Verlag, New York, 1983.